Small-angle X-ray scattering study of the phase structure of poly(D-(−)-3-hydroxybutyrate) and atactic poly(epichlorohydrin) blends

P. Sadocco*, M. Canetti and A. Seves
Stazione Sperimentale per la Cellulosa, Carta e Fibre Tessili Vegetali ed Artificiali, Piazza L. da Vinci 26, 20133 Milano, Italy

and E. Martuscelli
Istituto di Ricerche su Tecnologia dei Polimeri e Reologia del C.N.R., Via Toiano 6, 80072 Arco Felice (Napoli), Italy
(Received 12 May 1992; revised 26 October 1992)

Isothermally crystallized and annealed blends of poly(D-(−)-3-hydroxybutyrate) (PHB) and atactic poly(epichlorohydrin) (aPECH) were examined by wide-angle X-ray diffraction and small-angle X-ray scattering (WAXD and SAXS). The lateral crystal dimensions of PHB increased with annealing treatment and with increasing aPECH component in the blends, while the long-period distances of the blends were slightly smaller than for pure PHB. The scattering observed for the blends resulted from the superposition of the scattering arising from the crystalline regions (made up by alternate stacking of lamellae and thin amorphous layers) and from the aPECH inhomogeneity present outside them. The structural information was obtained, from the SAXS curves, on the basis of Glatter and Debye–Bueche approaches. The results suggest that, during melt-crystallization of PHB, segregation of aPECH occurs within the growing spherulite with its dispersion in the interfibrillar zones that are larger than the interlamellar regions but smaller than the overall spherulite. The aPECH molecules are dispersed at the molecular level in the interfibrillar zones where they can assume a random-coil conformation. The detection of a glass transition temperature (T_g) close to the aPECH T_g value indicates low interactions at the segmental level between the two polymers. The annealing treatment produced a general perfectioning and rearrangement of the sample morphology, enhancing the crystallinity and the crystal dimensions of PHB in the pure state and in the blends, and probably favouring the trend of the aPECH molecules to assume a globular conformation.

(Keywords: poly(hydroxybutyrate); poly(epichlorohydrin); blends; small-angle X-ray scattering; annealing; phase structure; crystal dimensions)

INTRODUCTION

A wide spectrum of morphologies is possible with semicrystalline–amorphous polymer mixtures and a proper evaluation of the properties of the mixtures requires an in-depth understanding of the different structures. The spherulitic structure of semicrystalline polymers consists of radiating arrays of fine crystalline fibrils and the spaces among them identify the interfibrillar zones. Each fibril contains the alternating layers of amorphous (interlamellar amorphous phase) and crystalline (lamellae) regions. Several blend systems have been examined in detail by small-angle X-ray scattering (SAXS) in order to obtain structural information about the localization of the amorphous component in the spherulitic structure of the crystalline polymer.

In the case of compatible blends of polycaprolactone/poly(vinyl chloride) (PCL/PVC)[1] and poly(ethylene oxide)/poly(methyl methacrylate) (PEO/PMMA)[2,3], the non-crystalline component was found to reside between the individual lamellae rather than in an interfibrillar or interspherulitic position. In fact, the thickness of the amorphous phase increased by increasing the content of the amorphous component, while the lamellar thickness did not vary, or in some cases increased (PEO/PMMA)[2], with composition.

For the isotactic polystyrene/poly(2,6-dimethylphenylene oxide) (iPS/PPO) compatible blend[4], the long period did not vary with blending, but it was demonstrated that the lamellar thickness decreases while the amorphous layer increases with increasing PPO content. These data show that the PPO resides in the interlamellar regions.

Different results were obtained by Warner *et al.*[5] in a study of blends of isotactic and atactic polystyrene (iPS/aPS). In this case the crystal thickness and amorphous layer thickness were independent of composition. The absence of segregation phenomena in the interspherulitic contact zones suggested that the

*To whom correspondence should be addressed

0032-3861/93/163368-08

non-crystallizable component was segregated in the interfibrillar zones, which are larger than the interlamellar zones but smaller than the spherulite.

For PEO/poly(vinyl acetate) blends[6], results somewhat intermediate of the above cases have been found. In fact, the morphological and structural properties of the blends were attributed to the presence of non-crystallizable material in both the interlamellar and interfibrillar regions.

The differences in behaviour of the above mentioned blends may be understood in terms of the parameter δ, defined by Keith and Padden[7] as $\delta = D/G$. This expression places the scale of segregation on a somewhat quantitative basis, where δ is the dimensional order of segregation, D is the diffusion coefficient of the non-crystallizing component in the crystallizing matrix, and G is the spherulitic radial growth rate. The parameter δ has dimensions of length and represents the distance that the rejected component may move during the time of crystallization. If δ is comparable with interlamellar distances, then the rejected component may reside between lamellae. Qualitatively, for example in the case of PCL/PVC, PEO/PMMA and iPS/PPO blends, the amorphous components have considerably higher values of T_g than the crystallizing polymer, and therefore the addition of the amorphous component predominantly decreases the diffusion term such that segregation occurs at the lamellar level. However, if D is larger, or G smaller, then δ may be sufficiently large that the rejected component resides in the larger domains within the spherulite (iPS/aPS).

The aim of the work presented in this paper was to derive information about the structure of blends of poly(D-(−)-3-hydroxybutyrate) (PHB) and atactic poly (epichlorohydrin) (aPECH) with the aid of SAXS and wide-angle X-ray diffraction (WAXD) techniques. The long period, crystal dimensions and crystallinity of pure PHB and PHB/aPECH blends, when isothermally crystallized and annealed, were investigated together with the aPECH distribution in the blends after PHB crystallization.

The crystallization and thermal behaviour of blends of PHB and aPECH have previously been studied[8]. The miscibility in the melt between the two polymers was evidenced by the influence of aPECH on the spherulitic growth rate and the overall crystallization rate of PHB, and by the detection of a single, composition-dependent glass transition temperature of the quenched blends. The depression of the equilibrium melting temperature, observed with blending, appeared to be strongly influenced by morphological effects.

EXPERIMENTAL

Materials

The poly(D-(−)-3-hydroxybutyrate) (ICI; $M_w = 166\,000$, $M_w/M_n = 2.85$) used was a semicrystalline powder isolated from *Alcaligenes eutrophus* cultures. Atactic poly(epichlorohydrin), i.e. poly(oxy-2-chloromethylethylene) (Aldrich; $M_w = 1\,078\,000$, $M_w/M_n = 3.52$), was purified by centrifugation and filtration of a dichloromethane solution. (The molecular weight data were obtained through gel permeation chromatography (g.p.c.) on a Waters GPC system.) The binary blends were prepared by solution casting from dichloromethane and then dried under vacuum at 80°C until they reached constant weight. Blends with weight ratios of 80/20, 60/40 and 40/60 PHB/aPECH were prepared. Blends and pure PHB were melted at 200°C for 2 min, then isothermally crystallized at 100°C. Then all the isothermally crystallized samples were annealed for 120 min at the annealing temperature (T_a) calculated as $T_a = T'_m - 19$°C (where T'_m is the apparent melting temperature). The T'_m values obtained by differential scanning calorimetry (d.s.c.) are in agreement with those reported in an earlier paper[8]. The details of the crystallization and annealing for each sample are reported in *Table 1*. Isothermally crystallized and annealed samples were analysed by d.s.c., WAXD and SAXS techniques.

Table 1 Times used for isothermal crystallization at 100°C (t) and annealing temperatures (T_a) for pure PHB and PHB/aPECH blends

PHB/aPECH	t (min)	T_a (°C)
100/0	30	141
80/20	40	140
60/40	55	136
40/40	227	131

Differential scanning calorimetry

The samples were analysed by a Perkin–Elmer DSC-4/Thermal Analysis Data Station (TADS). The samples (about 7 mg) were heated from −60 to 200°C at the two different scanning rates of 10 and 20°C min^{-1}. The glass transition temperature (T_g) was taken at the midpoint of the transition. The observed melting temperature (T'_m) was obtained from the maximum of the first endothermic peak. Gallium and indium standard samples were used to calibrate the instrument.

Wide-angle X-ray diffraction

X-ray diffraction measurements were made on a Siemens diffractometer model D-500 equipped with a Siemens FK 60-10, 2000 W Cu tube (CuKα_1 radiation, $\lambda = 1.54$ Å). The samples were mounted on a specimen carrier for specimen spinning. By spinning the sample about its surface normal the effect of preferred orientation could be eliminated. The rotational speed amounted to 30 r.p.m. The degree of crystallinity was calculated from diffracted intensity data in the range $2\theta = 11$–$40°$ by using the area integration method[9]. The method required that 100% amorphous polymer be available, then the diffracted intensity data of plain PHB and blends (quenched in liquid nitrogen) were employed to calculate the amorphous contribution. Lattice imperfections were not considered. The apparent crystal sizes were calculated from the line-broadening data collected with a scanning rate of 0.1 2θ deg min^{-1}. A nickel standard sample was employed to determine the instrumental broadening.

Small-angle X-ray scattering

SAXS data were measured at 25°C using a Huber 701 chamber[10] with a monochromator glass block. Monochromatized CuKα_1 X-rays ($\lambda = 1.54$ Å) were supplied by a stabilized Siemens Kristalloflex 710 generator and a Siemens FK 60-04, 1500 W Cu target tube. The scattered intensity was measured using a Siemens scintillator crystal and beryllium window. The intensity was counted at 85 angles of measurement in the range $2\theta = 0.1$–$3.8°$ with three different step intervals. To reduce the statistical

error of counting, for each sample the mean intensity values were obtained from 16 scans with a time of 21 h for a complete measurement. The standard deviations calculated for the intensity values at each counting angle showed a low degree of spread of the intensity data around the average values. The camera and the counting equipment were controlled by a Huber SCM 9000 interfaced with an Olivetti M 24 computer. The raw data were first corrected for sample absorption and then the background was subtracted.

For all SAXS measurements the abscissa variable Q was calculated from

$$Q = 4\pi(\sin\theta)/\lambda \quad (1)$$

The relation between the scattering intensity and the characteristic of a particle is given by the Fourier transformation

$$I(Q) = 4\pi \int_0^\infty p(r) \frac{\sin(Qr)}{Qr} \, dr \quad (2)$$

By the application of the indirect transformation method developed by Glatter[11,12], the three-dimensional distance distribution function $p(r)$ together with the corresponding propagated statistical error band can be calculated from unsmoothed and smeared experimental scattering data. The method consists of steps of smoothing, desmearing and transformation into real space, and the calculation of the scattering function that best approximates the experimental scattering profiles takes into account the experimental standard deviations (errors from counting statistics). For the desmearing the geometries of the incident beam profile and the detector were considered[11].

By application of the method to solid samples with a one-dimensional lamellar structure, the one-dimensional correlation function $\gamma(r)$ can be computed[12,13]. With the assumption of homogeneity along the basal plane of the lamella the scattering intensity can be written as the product

$$I(Q) = (2\pi A/Q^2) I_t(Q) \quad (3)$$

where A is the area of the lamella and $I_t(Q)$ is the one-dimensional scattering function. The connection between the one-dimensional scattering function and the one-dimensional correlation function $\gamma(r)$ is given by

$$I_t(Q) = 2 \int_0^\infty \gamma(r) \cos(Qr) \, dr \quad (4)$$

and the inverse transformation is

$$\gamma(r) = (1/\pi) \int_0^\infty I_t(Q) \cos(Qr) \, dQ \quad (5)$$

The one-dimensional correlation function shows a number of minima and maxima of decreasing height and finally becomes zero at large values of r due to the periodicity of the structure. The position of the first maximum then corresponds to the average value of the distance periodicity[14].

RESULTS AND DISCUSSION

Wide-angle X-ray diffraction

The data reported in *Table 2* show that the crystallinity X_c of the blends, as measured by WAXD, decreases with increasing aPECH content, while the crystallinity of the PHB component $X_{c(PHB)}$ is similar for pure PHB and 80/20 and 60/40 PHB/aPECH blends, and lower for the 40/60 blend. The annealing produces a general enhancement of the crystallinity and the $X_{c(PHB)}$ index reaches similar values for pure PHB and all blends.

Table 2 Crystalline weight fractions X_c and crystallinities of PHB component $X_{c(PHB)}$ obtained by WAXD for pure PHB and PHB/aPECH blends

	Isothermally crystallized		Annealed	
PHB/aPECH	X_c[a]	$X_{c(PHB)}$	X_c[a]	$X_{c(PHB)}$
100/0	0.54		0.65	
80/20	0.42	0.52	0.49	0.61
60/40	0.33	0.55	0.39	0.64
40/60	0.19	0.46	0.24	0.61

[a]The errors in the X_c values were calculated as ±4%

Table 3 Apparent crystal sizes D_{hkl} of pure PHB and PHB/aPECH blends (values in Å)[a]

	Isothermally crystallized			Annealed		
PHB/aPECH	(0 2 0)	(1 1 0)	(1 0 0)	(0 2 0)	(1 1 0)	(1 0 0)
100/0	208	152	223	254	202	333
80/20	271	158	194	289	228	371
60/40	289	211	309	352	276	567
40/60	284	234	413	323	301	830

[a]The errors in the D_{hkl} values were calculated as ±3%

The apparent crystal sizes D_{hkl} of PHB in the directions perpendicular to the (1 1 0) and (0 2 0) crystallographic planes were calculated by the Scherrer equation[9]

$$D_{hkl} = \frac{K\lambda}{\beta_0 \cos(\theta_{hkl})} \quad (6)$$

where β_0 is the half width in radians of the reflection corrected for instrumental broadening, and λ is the wavelength of the X-ray radiation employed (1.54 Å). The shape factor K is set equal to unity, and so the size data have to be considered as relative data[9].

The unit cell of PHB crystals is orthorhombic[15], and therefore the calculated dimensions allow the direct computation of the crystal growth along the b axis (D_{020}) and along the a axis by the trigonometrical extrapolation of the crystal size D_{100} in the direction perpendicular to the (1 0 0) crystallographic plane.

The (0 0 2) reflection relative to the (0 0 2) plane is disturbed by the overlapping of other diffractions, and therefore the crystal dimension along the c axis cannot be calculated.

The lateral crystal sizes of PHB increase with increasing aPECH fraction in the blends (*Table 3*). This fact may be justified by the decreased PHB crystallization rate in the presence of aPECH. In fact, the choice of a constant crystallization temperature (100°C) enhanced the time of crystallization with increasing aPECH fraction[8].

The annealing treatment increases the above mentioned crystal dimensions and the aPECH presence seems not to interfere with the lateral increment of PHB crystal dimensions (as can be observed for the 40/60 PHB/aPECH blend). It must be pointed out that for all samples the annealing temperature was uniformly chosen as 19°C lower than the apparent melting temperature and the time of treatment was kept constant.

Differential scanning calorimetry

In earlier work[8] the d.s.c. analyses conducted on pure PHB and PHB/aPECH blends, quenched from the melt to −200°C, gave single glass transition temperatures (T_g) with numerical values dependent on composition and in good agreement with the theoretical values derived by Fox[16]. These results were taken as an indication that the two polymers are miscible in the melt at the molecular level.

When observed under the optical polarizing microscope, the blends isothermally crystallized at 100°C appear to be completely filled with impinged spherulites. The absence of separate aPECH domains, both in the intraspherulitic regions and in the interspherulitic contact zones, suggests that the uncrystallizable component is incorporated in the interfibrillar and/or the interlamellar zones of PHB spherulites. D.s.c. scans conducted for pure PHB and blends, isothermally crystallized at 100°C, showed that for pure PHB the T_g of 4°C was no longer detectable[8], while for the blends a single glass transition appeared at a temperature value close to the pure aPECH T_g of −20°C. The T_g event was more pronounced with increasing aPECH fraction (*Figure 1*).

Small-angle X-ray scattering

Typical plots of background-subtracted SAXS intensity profiles for pure PHB and blends isothermally crystallized are shown in *Figure 2*. The presence of a

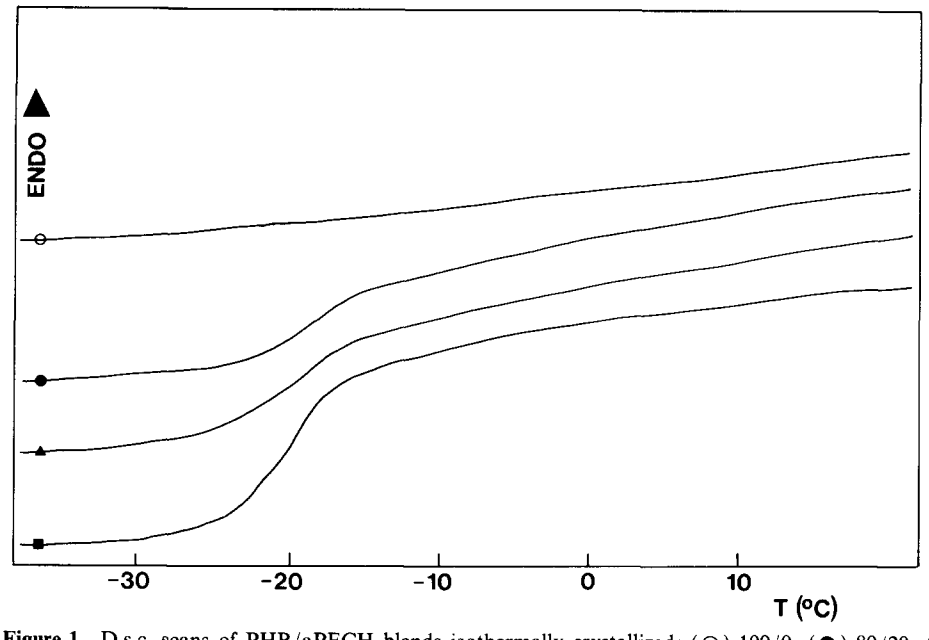

Figure 1 D.s.c. scans of PHB/aPECH blends isothermally crystallized: (○) 100/0; (●) 80/20; (▲) 60/40; (■) 40/60

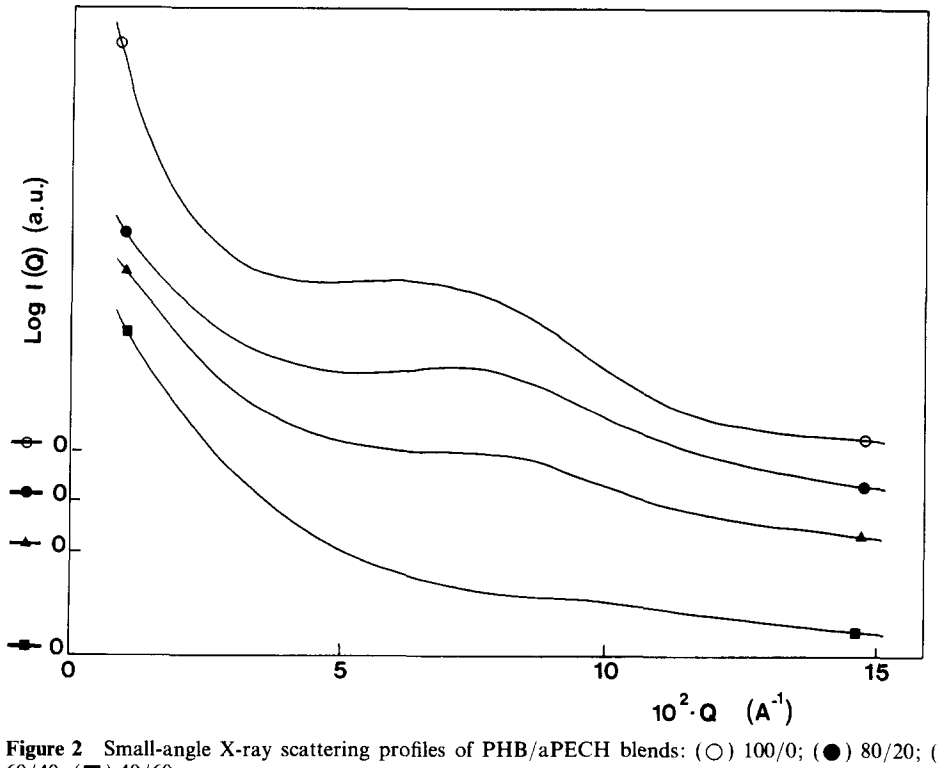

Figure 2 Small-angle X-ray scattering profiles of PHB/aPECH blends: (○) 100/0; (●) 80/20; (▲) 60/40; (■) 40/60

maximum can be observed in the scattering profiles, and the maximum becomes less pronounced with increasing aPECH concentration. With the 40/60 PHB/aPECH ratio no maximum was observable. The maxima are associated with the long period resulting from the presence of a macrolattice formed by the centres of adjacent lamellae. No shifts of the position of the maximum towards lower Q values were observed for blend samples.

The one-dimensional correlation functions were calculated for pure PHB and PHB/aPECH blends isothermally crystallized at 100°C (*Figure 3a*). The absence of a plateau in the region of the first minimum of the $\gamma(r)$ function makes it difficult to determine the structural parameters such as amorphous and crystalline lamellar thickness. It has been noted by several authors[17,18] that for samples of medium crystallinity ($0.3 < X_c < 0.7$) the evaluation of the scattering curve is inherently difficult and insensitive, and the calculated correlation function varies very little with X_c. As can be observed in *Table 2*, the X_c values of our samples fall in the critical range of insensitive SAXS data. Besides, the structural data obtainable from $\gamma(r)$ are compromised

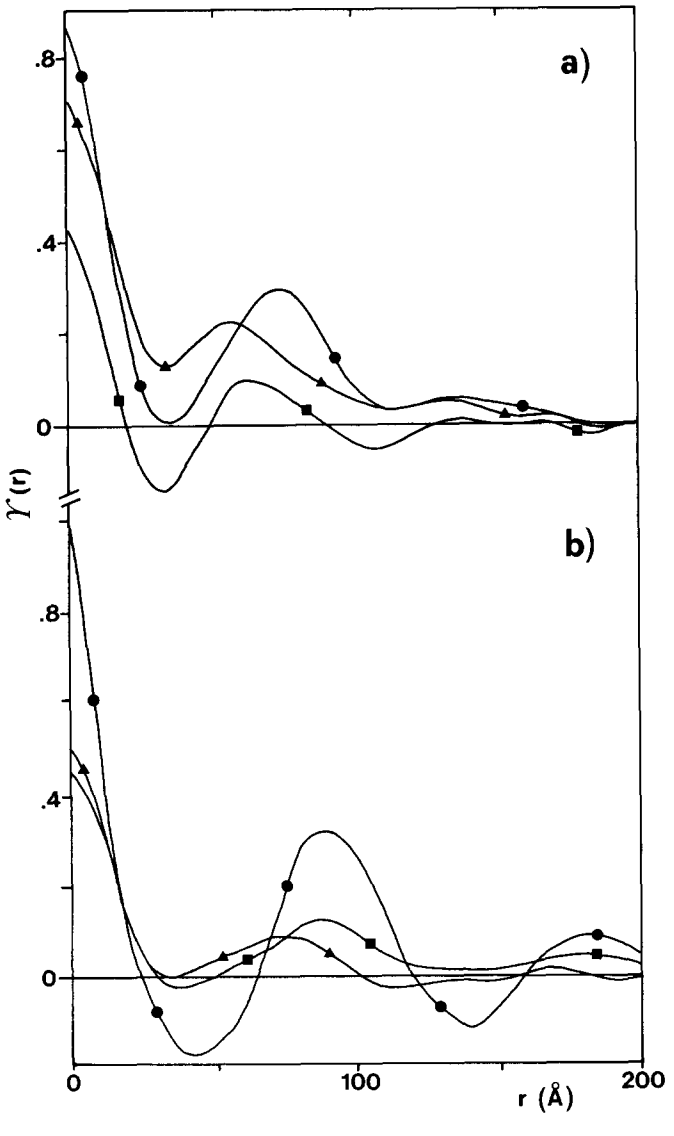

Figure 3 One-dimensional correlation functions $\tau(r)$ of PHB/aPECH blends. (a) Isothermally crystallized and (b) annealed: (●) 100/0; (■) 80/20; (▲) 60/40

Table 4 Long-period distances of PHB and PHB/aPECH blends (Å)

	Isothermally crystallized		Annealed	
PHB/aPECH	Lorentz[a]	$\gamma(r)$	Lorentz[a]	$\gamma(r)$
100/0	79	74±5	93	90±5
80/20	72	66±6	93	90±6
60/40	72	58±6	82	75±7
40/60	–	–	–	–

[a]The errors in the Lorentz long-period values were calculated as ±4%

owing to the presence of scattering arising from the inhomogeneity in the system, as will be discussed later on.

As can be observed in *Figure 3a* the correlation function of isothermally crystallized pure PHB is broad and broadens further on addition of aPECH. For the 40/60 PHB/aPECH blend the experimental intensity function could not be fitted with a one-dimensional approach.

The correlation functions of pure PHB and PHB/aPECH annealed blends are plotted in *Figure 3b*. For the annealed, pure PHB the $\gamma(r)$ profile is better defined than for the isothermally crystallized sample (*Figure 3a*), and a second maximum appears at an r value twice that at the first maximum. The increase in crystallinity and crystal perfectioning with annealing of PHB are in fact reproduced by the $\gamma(r)$ profile. For the 80/20 and 60/40 PHB/aPECH annealed blends the $\gamma(r)$ profiles are even more broad than the profiles of the corresponding non-annealed samples. The behaviour of the 40/60 PHB/aPECH annealed blend was similar to that of the isothermally crystallized sample.

From the position of the first maximum for each $\gamma(r)$ function the long period L was obtained, and these are reported in *Table 4* for the isothermally crystallized and annealed samples. Since the maxima are quite broad the L values so obtained must be considered only as indicative values.

After desmearing the intensities were Lorentz corrected and more accurate L values were calculated from

$$L = 2\pi/Qm \tag{7}$$

where Qm is the abscissa value at the maximum of the plot (*Figure 4a*). For the isothermally crystallized 80/20 and 60/40 blends, with respect to pure PHB the peak position slightly shifts towards higher Q values and the peak broadens as more aPECH is added to PHB. For the 40/60 PHB/aPECH blend the peak does not appear at all.

In *Figure 4b* the Lorentz plots of the annealed samples are shown. It can be observed that annealing produces an enhancement and a better resolution of the peak for pure PHB, while for blends the peak resolution does not improve at all.

In *Table 4* the L values obtained from the Lorentz plots and $\gamma(r)$ profiles are reported for the isothermally crystallized and annealed samples. The L values obtained from the $\gamma(r)$ profiles are lower than those obtained from the Lorentz plots but they have the same trend with respect to the blend composition and the annealing treatment. A general enhancement of the long-period values can be observed as a consequence of the annealing treatment and for the blend samples the long-period distance remains slightly lower than that of pure PHB.

The fact that the L values do not increase but are

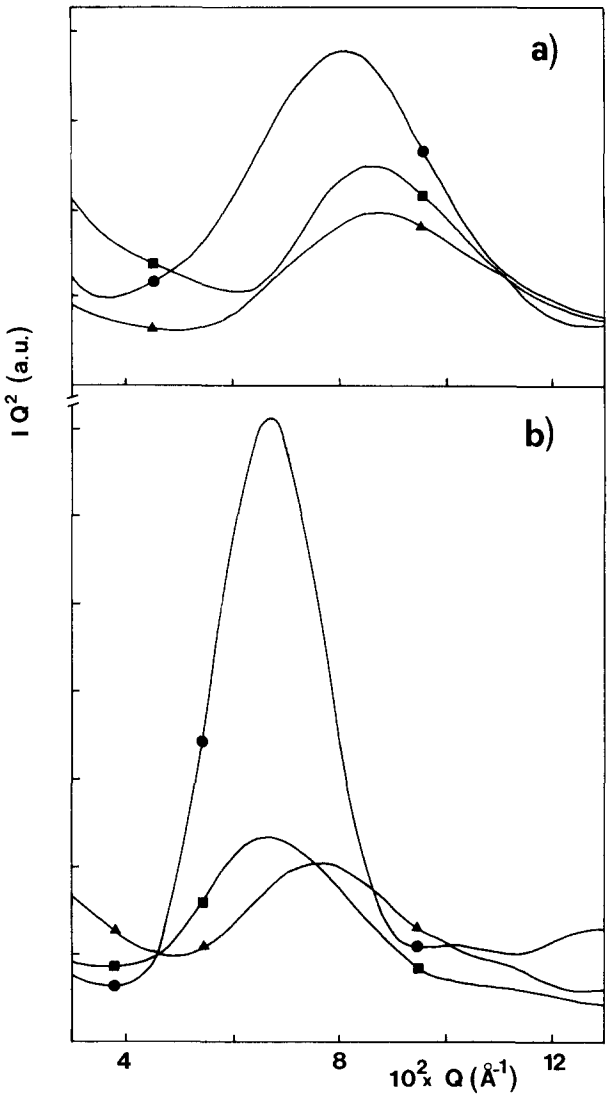

Figure 4 Lorentz plots of PHB/aPECH blends. (a) Isothermally crystallized and (b) annealed: (●) 100/0; (■) 80/20; (▲) 60/40

actually slightly lower for blends than for pure PHB supports the hypothesis that the aPECH is absent from the interlamellar PHB zones. The presence of aPECH in those regions could only be indicated by a very low PHB lamellar thickening with blending, which is very unlikely given the crystallinity and lateral crystal dimension data obtained by WAXD. In fact, when isothermally crystallized, the PHB component reached about the same crystallinity value with blending as in the pure state. Besides, it was observed that the lateral crystal sizes of PHB increased with blending.

Optical microscopy has shown the system to be completely volume filled with spherulites, and no segregation of the aPECH component was observed in the interspherulitic contact zones. This last observation together with the above discussion suggests that the non-crystallized component is segregated in the interfibrillar zones, which are larger than the interlamellar regions but smaller than the overall spherulite. To explain the scale of rejection of aPECH in the PHB crystallizing matrix during crystallization from the melt, the Keith and Padden[7] equation can be used, i.e. $\delta = D/G$. The presence of aPECH decreases the PHB spherulite growth rate[8] G, and the aPECH T_g value is lower than that of crystallizing PHB (aPECH $T_g = -20°C$, PHB $T_g = +4°C$). These facts give a relatively high diffusion term D in the δ parameter. The aPECH molecules diffuse away from the front of the PHB crystallization at such a rate so as not to remain segregated between lamellae, but in any case the mobility of aPECH is not sufficient to let it move away from the spherulites. Thus, aPECH will reside in the interfibrillar zones.

Considering the high aPECH M_w value, a monomolecular dispersion in the interfibrillar zones of aPECH molecules with a random-coil conformation can produce scattering. In fact, the volume filled by one molecule of aPECH having a weight-average molecular weight of 1 078 000 and a specific volume of 0.735 cm^3 g^{-1} has been deduced, and by the assumption of spherical shape a radius of about 70 Å was calculated.

The presence of scattering arising from the dispersed aPECH molecules finds a first confirmation in the results obtained from the annealed samples. As demonstrated by WAXD investigations about the crystallinity and crystal dimensions of PHB, the annealing treatment produces for pure PHB and blends a rearrangement and perfectioning of the crystalline region. In fact, for pure PHB the profiles of the one-dimensional correlation function $\gamma(r)$ and the one-dimensional scattering function (Lorentz plot) were better resolved after the annealing treatment. However, for the 80/20 and 60/40 blends an increase in broadness of the one-dimensional functions was observed after the annealing treatment (*Figures 3* and *4*). This poorer resolution with the one-dimensional approach can be explained by the interference of the scattering arising from aPECH molecules dispersed in the interfibrillar zones, and this interference seems to increase with the annealing treatment.

In the case of the 40/60 PHB/aPECH blend, for both isothermally crystallized and annealed samples the contribution to the scattering of the aPECH inhomogeneity in the system is such that the application of a one-dimensional approach to the experimental scattering profile is compromised.

In order to analyse the scattering arising from the presence of aPECH in the interfibrillar zones of blends the Debye–Bueche relation was used. This relation is generally applicable to the scattering intensity from the electron density fluctuation of an inhomogeneous system. The intensity $I(Q)$ is given by[19]

$$I(Q) = K_3 \langle n^2 \rangle l_c^3 [1 + Q^2 l_c^2]^{-2} \quad (8)$$

where $\langle n^2 \rangle$ is the mean-square density fluctuation in the system, l_c is the correlation length of the fluctuation and K_3 is a proportionality constant. Equation (8) can be rewritten as

$$[I(Q)]^{-1/2} = [K_3 \langle n^2 \rangle l_c^3]^{-1/2} [1 + Q^2 l_c^2] \quad (9)$$

For the scattering from an inhomogeneous system with correlation length l_c, $[I(Q)]^{-1/2}$ is linear when plotted against Q^2 and l_c^2 can be estimated from the ratio of slope to intercept.

In *Figure 5* the Debye–Bueche plots for blend samples are given. It can be observed that at small Q^2 values the plots are nearly linear and they deviate from linearity at larger Q^2. The deviation is caused by the addition of the scattering from the crystalline–amorphous region, while the linearity at smaller Q^2 represents scattering due to the inhomogeneity of the system[20]. In fact, for the isothermally crystallized blends the linearity continues to larger Q^2 as the PHB fraction decreases, giving the indication that in the blends besides the crystalline region

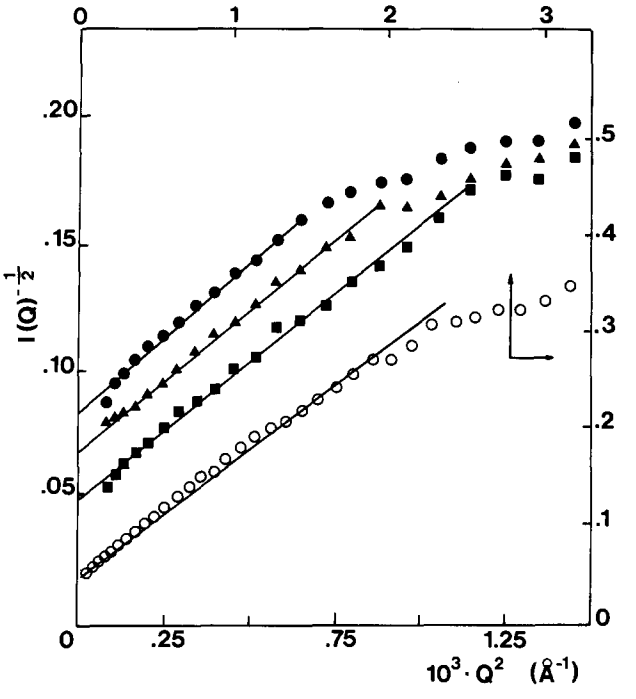

Figure 5 Debye–Bueche plots of PHB/aPECH blends. Isothermally crystallized: (●) 80/20; (▲) 60/40; (■) 40/60. Annealed: (○) 40/60. The axes of this last curve are indicated by the arrows

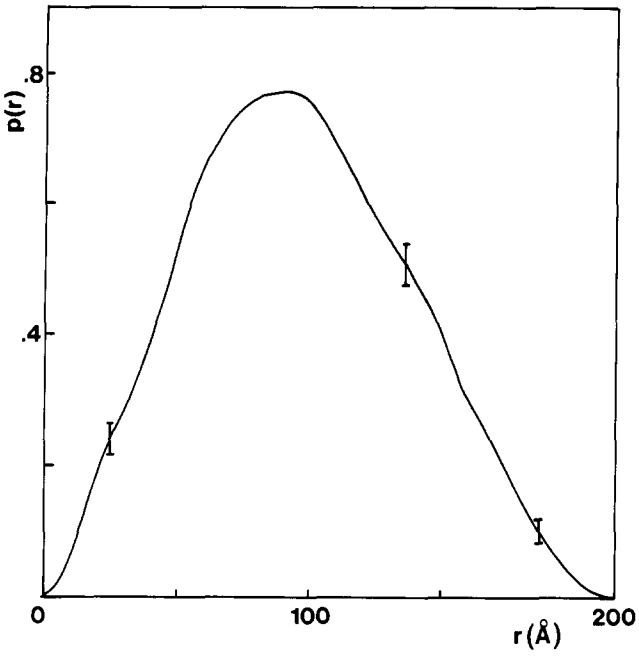

Figure 6 Three-dimensional distance distribution function $p(r)$ for the isothermally crystallized 40/60 PHB/aPECH blend

there exists some amorphous inhomogeneity. In *Figure 5* the curve of the 40/60 annealed blend is also shown and it can be noted that the linearity continues to a Q^2 value higher than that for the 40/60 isothermally crystallized blend. The contribution of aPECH to the scattering increases as a consequence of the annealing treatment.

The l_c values calculated for all blends do not significantly vary with the aPECH content or annealing treatment; the average of the obtained l_c is 45 ± 5 Å. These results indicate that no aggregation phenomena occur with increasing aPECH content in the blends.

For the 40/60 blends, which showed a greater contribution by aPECH to the scattering and for which the one-dimensional approach failed, a three-dimensional analysis of the scattering profile was conducted with the computation of the three-dimensional distance distribution function $p(r)$[11,12]. Gaussian curves were obtained, indicating that the scattering is due to globular particles of aPECH (*Figure 6*) and there was a good correlation between the scattering profiles approximated by the program and the experimental results[11].

The radius of gyration of the whole particle R_g was calculated from the $p(r)$ function[11,12] using

$$R_g^2 = \frac{\int_0^\infty p(r) r^2 \, dr}{2 \int_0^\infty p(r) \, dr} \tag{10}$$

The R_g values obtained were about 70 Å for both 40/60 isothermally crystallized and 40/60 annealed blends. These values give a measure of the dispersion of aPECH molecules with globular symmetry in the interfibrillar zones, and with reference to the aforementioned calculated dimensions of a single aPECH molecule, aPECH appears to be dispersed at the molecular level. It must be pointed out that the polydispersity of the system and the difficulties in separating the scattering that arises from the crystalline region make the experimental measure of aPECH dispersion merely an indicator of the order of magnitude of dispersion.

CONCLUSIONS

After PHB crystallization from the melt the aPECH molecules are rejected into the interfibrillar zones where they are dispersed at the molecular level and where they probably assume a random-coil conformation. In spite of the molecular dispersion of aPECH, the detection for the blends of a T_g value close to the T_g of aPECH indicates weak interactions at the segmental level between the two polymers. The trend of aPECH molecules to assume a random-coil conformation together with the high M_w can hinder the close contact between aPECH and PHB molecules in the continuous interfibrillar zone.

The annealing treatment promotes a general perfectioning and rearrangement of the sample morphology, enhancing the crystallinity and the crystal dimensions of PHB in the pure state and in the blends, and probably favouring the trend of the aPECH molecules to assume a globular conformation.

ACKNOWLEDGEMENT

This work was partly supported by Progretto Finalizzato Chimica Fine del C.N.R.

REFERENCES

1 Khambatta, F. B., Warner, F., Russel, T. P. and Stein, R. S. *J. Polym. Sci., Polym. Phys. Edn* 1976, **14**, 1391
2 Silvestre, C., Cimmino, S., Martuscelli, E., Karasz, F. E. and MacKnight, W. J. *Polymer* 1986, **28**, 1190
3 Russel, T. P., Ito, H. and Wignall, G. *Macromolecules* 1988, **21**, 1703
4 Wenig, W., Karasz, F. E. and MacKnight, W. J. *J. Appl. Phys.* 1975, **46**, 4194
5 Warner, F. P., MacKnight, W. J. and Stein, R. S. *J. Polym. Sci., Polym. Phys. Edn* 1977, **15**, 2113
6 Silvestre, C., Karasz, F. E., MacKnight, W. J. and Martuscelli, E. *Eur. Polym. J.* 1987, **23**, 745

7 Keith, H. D. and Padden, F. J. *J. Appl. Phys.* 1964, **35**(4), 1270
8 Dubini Paglia, E., Beltrame, P. L., Canetti, M., Seves, A., Marcandalli, B. and Martuscelli, E. *Polymer* 1993, **34**, 996
9 Alexander, L. E., 'X-ray Diffraction Methods in Polymer Science', Wiley-Interscience, New York, 1969, p. 137
10 Schnabel, E., Hosemann, R. and Rode, B. *J. Appl. Phys.* 1972, **43**, 3237
11 Glatter, O. *J. Appl. Cryst.* 1977, **10**, 415
12 Glatter, O. and Kratky, O. 'Small Angle X-ray Scattering', Academic Press, London, 1982, p. 119
13 Glatter, O. *J. Appl. Cryst.* 1980, **13**, 577
14 Vonk, C. G. and Kortleve, G. *Koll. Z. Z. Polym.* 1967, **220**, 19
15 Yokouchi, M., Chatani, Y., Tadokoro, H., Teranishi, K. and Tani, H. *Polymer* 1973, **14**, 267
16 Fox, T. G. *Bull. Am. Phys. Soc.* 1956, **2**, 123
17 Strobl, G. R. and Schneider, M. *J. Polym. Sci., Polym. Phys. Edn* 1980, **18**, 1343
18 Kortleve, G. and Vonk, C. G. *Koll. Z. Z. Polym.* 1968, **225**, 124
19 Debye, P. and Bueche, A. M. *J. Appl. Phys.* 1949, **20**, 518
20 Nojima, S., Terashima, Y. and Ashida, T. *Polymer* 1986, **27**, 1007